

Mucin Secretion Induced by Titanium Dioxide Nanoparticles

Eric Y. T. Chen¹, Maria Garnica¹, Yung-Chen Wang, Chi-Shuo Chen, Wei-Chun Chin*

Bioengineering, University of California Merced, Merced, California, United States of America

Abstract

Nanoparticle (NP) exposure has been closely associated with the exacerbation and pathophysiology of many respiratory diseases such as Chronic Obstructive Pulmonary Disease (COPD) and asthma. Mucus hypersecretion and accumulation in the airway are major clinical manifestations commonly found in these diseases. Among a broad spectrum of NPs, titanium dioxide (TiO₂), one of the PM10 components, is widely utilized in the nanoindustry for manufacturing and processing of various commercial products. Although TiO₂ NPs have been shown to induce cellular nanotoxicity and emphysema-like symptoms, whether TiO₂ NPs can directly induce mucus secretion from airway cells is currently unknown. Herein, we showed that TiO₂ NPs (<75 nm) can directly stimulate mucin secretion from human bronchial ChaGo-K1 epithelial cells via a Ca²⁺ signaling mediated pathway. The amount of mucin secreted was quantified with enzyme-linked lectin assay (ELLA). The corresponding changes in cytosolic Ca²⁺ concentration were monitored with Rhod-2, a fluorescent Ca²⁺ dye. We found that TiO₂ NP-evoked mucin secretion was a function of increasing intracellular Ca²⁺ concentration resulting from an extracellular Ca²⁺ influx via membrane Ca²⁺ channels and cytosolic ER Ca²⁺ release. The calcium-induced calcium release (CICR) mechanism played a major role in further amplifying the intracellular Ca²⁺ signal and in sustaining a cytosolic Ca²⁺ increase. This study provides a potential mechanistic link between airborne NPs and the pathoetiology of pulmonary diseases involving mucus hypersecretion.

Citation: Chen EYT, Garnica M, Wang Y-C, Chen C-S, Chin W-C (2011) Mucin Secretion Induced by Titanium Dioxide Nanoparticles. PLoS ONE 6(1): e16198. doi:10.1371/journal.pone.0016198

Editor: Meni Wanunu, University of Pennsylvania, United States of America

Received: September 20, 2010; **Accepted:** December 7, 2010; **Published:** January 19, 2011

Copyright: © 2011 Chen et al. This is an open-access article distributed under the terms of the Creative Commons Attribution License, which permits unrestricted use, distribution, and reproduction in any medium, provided the original author and source are credited.

Funding: This study was supported by grants from NIH (1R15HL095039), NSF (CBET-0932404) and the UC CITRIS Program. CSC was supported by UC Merced Center of Excellence on Health Disparities (1P20MD005049-01 from the National Center on Minority Health and Health Disparities). EYTC was supported by GRC summer fellowship from UC Merced. The funders had no role in study design, data collection and analysis, decision to publish, or preparation of the manuscript.

Competing Interests: Dr. Chin is a member of the editorial board of PLoS ONE. This does not alter the authors' adherence to all the PLoS ONE policies on sharing data and materials.

* E-mail: wchin2@ucmerced.edu

These authors contributed equally to this work.

Introduction

Many published reports have demonstrated the association between NP exposure and pulmonary morbidity and mortality [1,2,3]. The adverse effects induced by NPs seem to exacerbate clinical symptoms of pre-existing respiratory illnesses such as asthma, COPD and Cystic Fibrosis (CF) [1,2,3,4,5,6]. During NP exposure, individuals with respiratory diseases showed more incidences of bronchoconstriction, medication use, bronchial hyperreactivity and lung fibrosis [2,7]. TiO₂ NPs are widely used in the nanotechnology industry due to their vast array of applications that range from household commodities, such as components of paints and carpets, to personal products that include cosmetics, textiles, sunscreens and foods [8,9]. TiO₂ is also one of the PM10 components commonly found in industries or manufacturing plants involved in processing mineral ore rutile [10]. It has been reported that >50% of TiO₂ NP exposed workers had respiratory symptoms accompanied by reduction in pulmonary function [10,11]. Other reports have also indicated that inhalation of TiO₂ NPs can induce pulmonary inflammatory responses (characterized by neutrophil recruitment), epithelial cell death and increased permeability [2,9]. Furthermore, TiO₂ NPs have been shown to play a role in inducing epithelial fibroproliferative changes, stimulating goblet cell hyperplasia and in instigating emphysema-like (such as alveolar enlargement) damages

in the lungs [2,10,12]. Overall, nanotoxicity induced by TiO₂ NP exposure in both the occupational and ambient environment presents a significant and realistic health concern.

The harmful effects of NPs on the respiratory system not only encompass cellular apoptosis/necrosis, but also mucus hyperproduction which is closely associated with the pathogenesis of pulmonary diseases that include asthma, COPD and CF [2,10,13]. In these chronic pulmonary diseases, mucus hypersecretion and accumulation may lead to recurrent episodes of chronic bacterial infections, limited airflow and chronic inflammatory responses [2,14,15]. However, whether TiO₂ NPs can directly induce mucin secretion has not been resolved.

Airway mucus plays a vital role in the constant clearance of inhaled pathogens and particulates. Mucus is a large, highly glycosylated protein consisting of an array of mucin peptides (apomucin) [14]. With their oligosaccharide sidegroups, such as sialic acid, sulfate, and carboxyl (COO⁻), mucins are usually polyanionic in nature [16]. Mucin secretion is closely regulated by cytosolic Ca²⁺ concentrations ([Ca²⁺]_C) in various epithelial cells [17]. A rise in [Ca²⁺]_C is crucial for initiating a cascade of downstream events including the mobilization of granule-bound Ca²⁺, docking of the secretory granules, fusion of the plasma-granule membrane and the formation of secretory pores, therefore leading to the exocytosis of the mucin granules [18].

Agonist-induced opening of various Ca^{2+} channels expressed on the cell membrane allows the influx of extracellular Ca^{2+} , which may serve as the external Ca^{2+} source [19]. The initial upsurge in the $[\text{Ca}^{2+}]_C$ is usually relayed by triggering a secondary wave of Ca^{2+} propagation from internal stores, such as the ER [19,20,21,22]. Ryanodine receptors (RYRs) on the ER have multiple allosteric Ca^{2+} binding sites responsible for triggering Ca^{2+} -induced Ca^{2+} release (CICR) into the cytosol [19,20,21,22]. The resultant increase in $[\text{Ca}^{2+}]_C$ could activate other cytosolic proteins and modulate secretion of mucin, hormones or various neurotransmitters [17,23,24].

NPs have been shown to disturb cellular functions by elevating intracellular Ca^{2+} levels [25,26,27,28]. For example, ultrafine carbon black NPs can elicit Ca^{2+} -dependent secretion through the activation of L-type voltage-gated Ca^{2+} channels [25,26,28]. However, little is known regarding the intricate calcium signaling pathway regulating the exocytotic events of secretory products. In this study, we aim to investigate the mechanism through which TiO_2 NPs induce mucin secretion via a Ca^{2+} signaling mediated pathway.

Materials and Methods

1. Culture of ChaGo-K1 cells

The human airway bronchial epithelial cell line ChaGo-K1, obtained from American Type Culture Collection (ATCC, Manassas, VA, USA), was used because it expresses MUC proteins and secretes mucin [29]. Cells were cultured in 15 cm cell culture plates (VWR, CA, USA) in RPMI 1640 medium (Invitrogen, CA, USA) supplemented with L-glutamine, 1% penicillin/streptomycin and 10% heat inactivated fetal bovine serum (FBS). Cultures were incubated in a humidified incubator at $37^\circ\text{C}/5\% \text{CO}_2$. Cell counts were performed using trypan blue (Sigma-Aldrich, MO, USA) exclusion and a Bright-Line haemocytometer.

2. Nanoparticles and characterization

A mixture of anatase and rutile forms of ultrafine titanium (IV) dioxide ($<75 \text{ nm}$) (Sigma-Aldrich, MO, USA) was used in this study because this form has been shown to result in more severe cellular injuries [30,31]. The TiO_2 NPs have a surface area of $36 \text{ m}^2/\text{g}$ and the dispersion conductivity is $1040 \mu\text{S}/\text{cm}$ (information from Sigma). All NP samples were sonicated before usage. The concentrations used were $1 \text{ mg}/\text{ml}$, $0.75 \text{ mg}/\text{ml}$, $0.5 \text{ mg}/\text{ml}$, $0.25 \text{ mg}/\text{ml}$, $0.1 \text{ mg}/\text{ml}$, and $0.05 \text{ mg}/\text{ml}$. The range of concentrations used was consistent with the concentrations of TiO_2 NPs found in previous reports [30]. The TiO_2 NPs were reconstituted with Hanks' solution (Invitrogen, CA, USA) before being tested. The size of NPs was independently confirmed using homodyne dynamics laser scattering (DLS) as described in previous studies [32,33].

3. Cell preparation

Cells were seeded at 2×10^5 cells per well in a 24-well plate, and incubated for 24 hrs in RPMI 1640 supplemented with 10% FBS. Following 24 hr incubation, the RPMI medium was removed from the cells and the culture was rinsed with Hanks' solution twice before use.

4. Measurements of cytosolic Ca^{2+} concentrations induced by TiO_2 exposure

The cells were then loaded with a Rhod-2 AM dye ($1 \mu\text{M}$) ($K_d = 570 \text{ nM}$, $\lambda_{\text{Ex}} = 552 \text{ nm}$ and $\lambda_{\text{Em}} = 581$) (Invitrogen, CA, USA) for 45 minutes. After the dye loading, the cells were rinsed,

incubated with either normal Hanks' or Ca^{2+} -free Hanks' solution, and treated with the appropriate TiO_2 concentrations. All calcium signaling experiments were carried out on a thermoregulated stage at 37°C mounted on a Nikon microscope (Nikon Eclipse TE2000-U, Tokyo, Japan). ChaGo-K1 cells were incubated with cadmium chloride ($200 \mu\text{M}$; Sigma-Aldrich, MO, USA) to block the membrane Ca^{2+} channels [34], followed by TiO_2 NP stimulation. To investigate the interaction between TiO_2 and membrane Ca^{2+} channels, nifedipine ($10 \mu\text{M}$; Sigma-Aldrich, MO, USA), an L-type Ca^{2+} channel blocker [27], was added to ChaGo-K1 cells prior to the exposure of TiO_2 . Antioxidant N-acetylcysteine (NAC, $250 \mu\text{M}$; Sigma-Aldrich, MO, USA) was also added to ChaGo-K1 cells to study the involvement of reactive oxygen species (ROS) [27,35], possibly generated as a result of TiO_2 stimulation, and the activation of Ca^{2+} channels. Thapsigargin (100 nM ; Sigma-Aldrich, MO, USA) [18] and ryanodine ($100 \mu\text{M}$; Sigma-Aldrich, MO, USA) were added separately to deplete the ER Ca^{2+} content and to inhibit the CICR mechanism [20,21], correspondingly. These two blockers were utilized to investigate the contribution from the internal ER Ca^{2+} pool.

5. Calcein dye leakage measurements

ChaGo-K1 cells were seeded at the density of 2×10^5 cells per well in a 24-well plate and cultured for 24 hrs. TiO_2 NP prepared with calcein fluorescent dye ($50 \mu\text{M}$) (Invitrogen, CA, USA) in Hanks' solution was incubated with the cells for 5 minutes at 37°C . Calcein is a biological inert green-fluorescent molecule of a molecular mass of 623 Da and an estimated molecular radius of 0.6 nm [36]. TiO_2 NP solution containing the calcein dye was then removed and cells were rinsed twice with PBS to remove possible remnants of calcein dye in the extracellular solution. The cells were subsequently stained with a fluorescent nucleus dye, hoechst ($10 \mu\text{M}$) (Sigma-Aldrich, MO, USA), for 5 minutes at 37°C and thoroughly rinsed again [33]. Fresh Hanks' solution was added into each well before taking fluorescent images of calcein and hoechst loaded cells with a Nikon fluorescence microscope. A percentage of calcein loaded cells against total number of cells, as indicated by hoechst fluorescence, was calculated for each of the TiO_2 NP concentrations used in the experiment.

6. Mucin secretion and ELLA Preparation

The cells were seeded at 2×10^5 cells per well in a 24-well plate and cultured for 24 hrs. ChaGo-K1 cells were then rinsed with PBS and treated with BAPTA-AM (Invitrogen, CA, USA), thapsigargin (Sigma-Aldrich, MO, USA) or ryanodine (Sigma-Aldrich, MO, USA) for at least 30 minutes. Afterward the cells were stimulated for 15 minutes with the corresponding TiO_2 NP concentrations ($0.75 \text{ mg}/\text{ml}$, $0.5 \text{ mg}/\text{ml}$, $0.25 \text{ mg}/\text{ml}$, and $0.1 \text{ mg}/\text{ml}$) or ionomycin ($1 \mu\text{M}$) (positive control) (Sigma-Aldrich, MO, USA), both prepared in PBS. The supernatant containing secreted mucin was collected and briefly centrifuged at $8,000 \text{ rpm}$ to remove the residual TiO_2 NPs. The supernatant was then incubated in a 96 well (Nunc MaxiSorp, VWR, CA, USA) plate overnight at 4°C . Afterward the 96-well plate was washed with PBST (PBS + 0.05% Tween-20) and then blocked with 1% BSA. The 96 well plate was washed again with PBST and incubated with lectin (Wheat germ agglutinin, WGA) (Sigma-Aldrich, MO, USA), conjugated to horseradish peroxidase (HRP; $5 \mu\text{g}/\text{ml}$) (Sigma-Aldrich, MO, USA), at 37°C for 1 hr. The substrate, 3,3',5,5'-Tetramethylbenzidine (TMB; Sigma-Aldrich, MO, USA), was added to each well at room temperature followed by H_2SO_4 (Sigma-Aldrich, MO, USA) in order to terminate the reaction. The optical density was measured at 450 nm [37].

7. Image Analysis

After staining the treated cells, image analysis was performed with an inverted Nikon Eclipse TE2000-U fluorescent microscope. Each photo was taken at a magnification of 200× and analyzed using SimplePCI (Compix Inc., Imaging Systems, Sewickle, PA, USA). The data shown is a representative of Ca^{2+} signals of more than 200 cells.

8. Statistical Analysis

The data was presented as means±SD. Each experiment was performed independently at least three times. Statistical significance was determined using a Student's t-test analysis with p values <0.05 (GraphPad Prism 4.0, GraphPad Software, Inc., San Diego, CA, USA).

Results

TiO₂ NP characterization

Dynamic laser scattering (DLS) was used to characterize the TiO₂ NPs. The particle size distribution ranged from ~9 to 80 nm due to minor aggregation or agglomeration while the predominant size is ~50 nm (Fig. 1A).

TiO₂ NPs induce cytosolic Ca²⁺ concentration increase

To investigate whether TiO₂ NPs could generate an increase in $[\text{Ca}^{2+}]_C$, ChaGo-K1 cells were loaded with Rhod-2 AM dye and exposed to 0.05–1 mg/ml of TiO₂ NPs. The change in $[\text{Ca}^{2+}]_C$, as represented by the fluorescence intensity within ChaGo-K1 cells, was monitored for 60 seconds. Figure 1B shows that 1 mg/ml of TiO₂ NPs induced an approximate 150% increase, while lower TiO₂ concentrations (<0.1 mg/ml) caused a minor elevation (~110%) in $[\text{Ca}^{2+}]_C$ when compared with untreated cells. The effect of TiO₂ treatment on the $[\text{Ca}^{2+}]_C$ of ChaGo-K1 cells followed a concentration-dependent manner (Fig. 1B).

Extracellular source for Ca²⁺ increase

To determine the main source of elevated $[\text{Ca}^{2+}]_C$ upon stimulation, ChaGo-K1 cells were exposed to TiO₂ NPs in Ca²⁺-free Hanks' solution. EGTA (2 mM) was added in Hanks' solution

to chelate possible traces of Ca²⁺. TiO₂ (0.05 mg/ml–1 mg/ml) treatment under Ca²⁺-free conditions failed to instigate a significant increase in $[\text{Ca}^{2+}]_C$ (Fig. 2A). Our data suggests that the extracellular Ca²⁺ pool is the primary source of the observed cytosolic Ca²⁺ increase. We then tested whether TiO₂ NPs can induce a Ca²⁺ influx via membrane channels. Blocking the channels with CdCl₂ (200 μM) significantly inhibited an increase in $[\text{Ca}^{2+}]_C$ (Fig. 2B). Co-treatment of cells with TiO₂ NPs and nifedipine greatly blocked the NP-induced $[\text{Ca}^{2+}]_C$ increase (Fig. 2C). However, the incomplete blockage of extracellular Ca²⁺ influx via channels postulates additional Ca²⁺ leakage through perturbed cell membranes. To confirm whether TiO₂ can instigate membrane disruption, thereby permitting unspecific extracellular Ca²⁺ entry, cytosolic leakage was assessed using the fluorescent calcein dye. It was found that the dye permeation ratio increased from approximately 4 to 13% with elevated TiO₂ concentrations ranging from 0.1 to 1 mg/ml (Fig. 2D).

Oxidative stress induced Ca²⁺ influx

To demonstrate that TiO₂-evoked $[\text{Ca}^{2+}]_C$ increase can be associated with oxidative stress, cells were pretreated with an antioxidant, N-acetylcysteine (NAC) [27]. Pre-treatment with NAC was able to partially attenuate the increase in cytosolic Ca²⁺ level triggered by 1 mg/ml and 0.75 mg/ml TiO₂ exposure (Fig. 2E). These results support the idea that oxidative stress, induced by TiO₂ NPs, contributes to the observed $[\text{Ca}^{2+}]_C$ increase and promote Ca²⁺-dependent mucin secretion.

The ER as an intracellular source of Ca²⁺

In order to determine the involvement of ER Ca²⁺ pool, it was depleted by pre-incubating the cells with thapsigargin. Pre-treatment with thapsigargin impeded TiO₂ NPs from triggering a sustained increase in the cytosolic Ca²⁺ level (Fig. 3A). We then investigated the role of the CICR mechanism by blocking RYRs (ryanodine receptors) [20]. Our results revealed that CICR was largely inhibited by ryanodine (a blocker for RYR associated with the CICR response) resulting in a significantly diminished $[\text{Ca}^{2+}]_C$ increase induced by NPs (Fig. 3B).

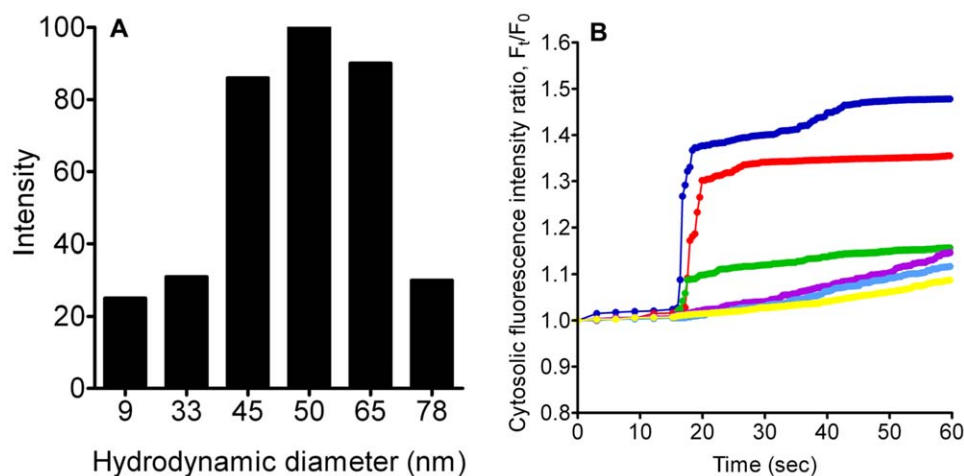


Figure 1. TiO₂ NP characterization and resultant $[\text{Ca}^{2+}]_C$ changes after NP treatment. A) DLS assessment of TiO₂ NPs in Hanks' solution showed a size distribution of ~9 to 80 nm. B) Cells were treated with TiO₂ NPs with concentrations of 0.05 mg/ml (yellow), 0.1 mg/ml (Light Blue), 0.25 mg/ml (Purple), 0.5 mg/ml (Green), 0.75 mg/ml (Red), and 1 mg/ml (Blue) in normal Hanks' solution. Each line represents the average fluorescence intensity of approximately 200 cells per well. doi:10.1371/journal.pone.0016198.g001

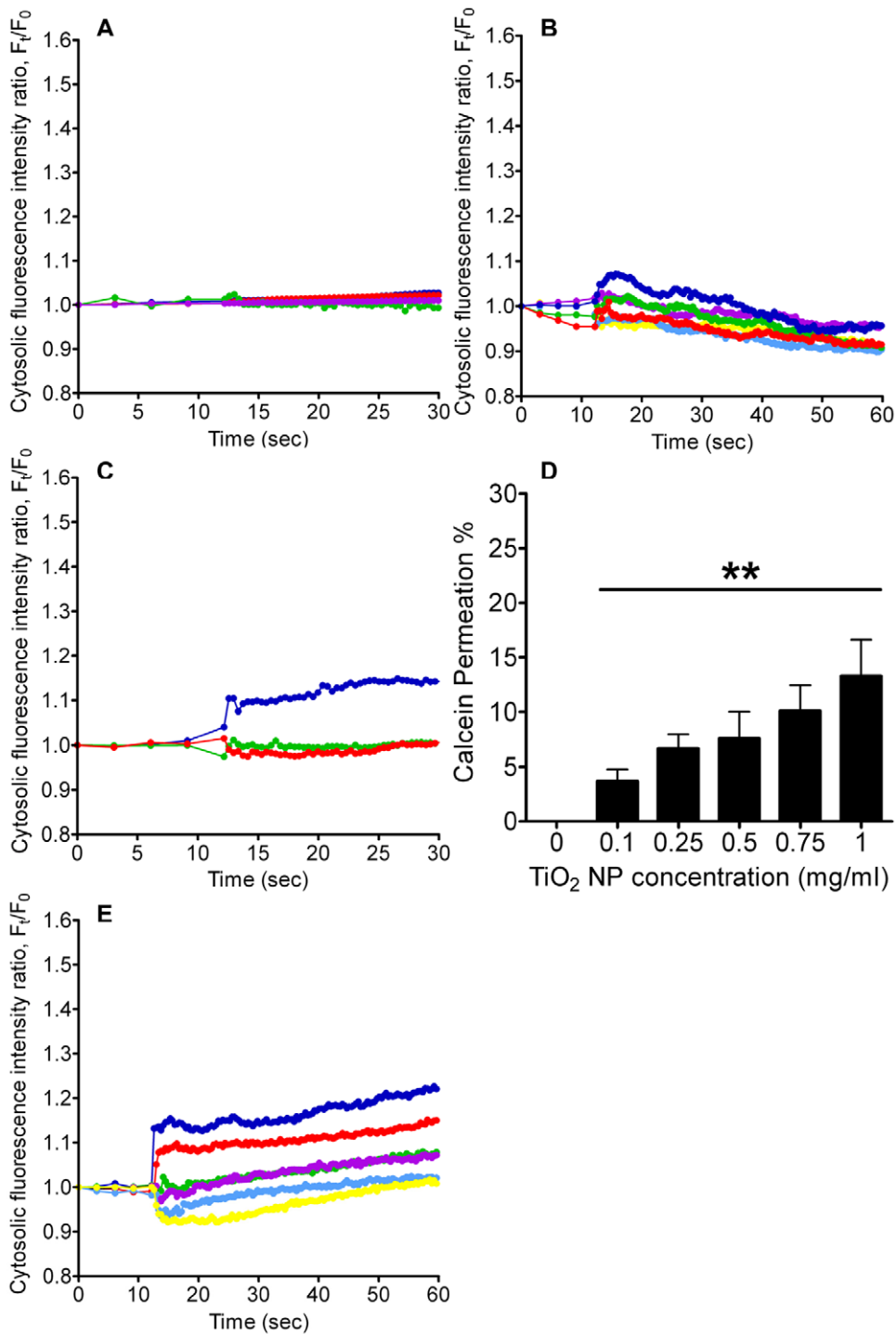


Figure 2. Measurement of the $[Ca^{2+}]_c$ and calcein dye leakage after TiO₂ NP treatment. Cells were treated with TiO₂ NPs with concentrations ranging from 0.05 mg/ml–1 mg/ml, in A) Ca²⁺-free Hanks' solution, B) in the presence of CdCl₂ (200 μM), C) nifedipine (10 μM), D) calcein (50 μM) (n = 12, **P < 0.005), and E) NAC (250 μM) (colors are as depicted in Figure 1B). doi:10.1371/journal.pone.0016198.g002

Ca²⁺-dependency of TiO₂-induced mucin secretion

Enzyme-linked lectin assay (ELLA) was used to assess the amount of mucin secreted from ChaGo-K1 cells when stimulated with TiO₂ NPs. When compared to the control, TiO₂ NPs increased mucin secretion by 113%, 125%, 133%, 137% and 150% at 0.05, 0.1, 0.25, 0.5 and 0.75 mg/ml, respectively (Fig. 4A). Chelating the intracellular Ca²⁺ with BAPTA-AM

yielded a significant reduction in mucin secretion (Fig. 4B). Addition of thapsigargin (Fig. 4C) or ryanodine (Fig. 4D) also resulted in diminished mucin secretion induced by TiO₂ NPs. Our data indicates that TiO₂-induced mucin secretion is dependent on the $[Ca^{2+}]_c$, attributed to both external and internal Ca²⁺ pools (Fig. 4A–D). Ionomycin (a Ca²⁺ ionophore) was used to elicit mucin secretion as a positive control (Fig. 5).

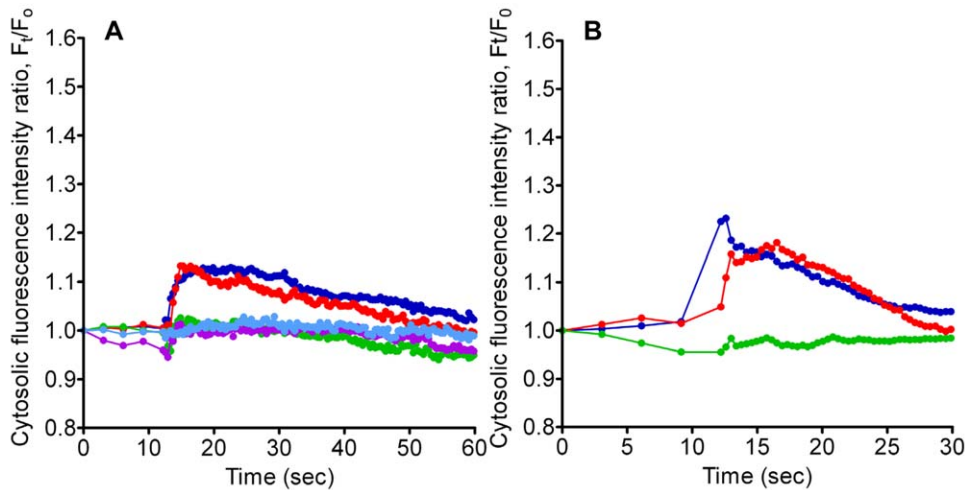


Figure 3. Measurement of $[Ca^{2+}]_C$ after stimulation by TiO_2 NPs. Cells were treated with TiO_2 NPs with concentrations ranging from 0.1 mg/ml –1 mg/ml, in the presence of A) thapsigargin (100 nM), and B) ryanodine (100 μ M) (colors used are consistent with Figure 1). doi:10.1371/journal.pone.0016198.g003

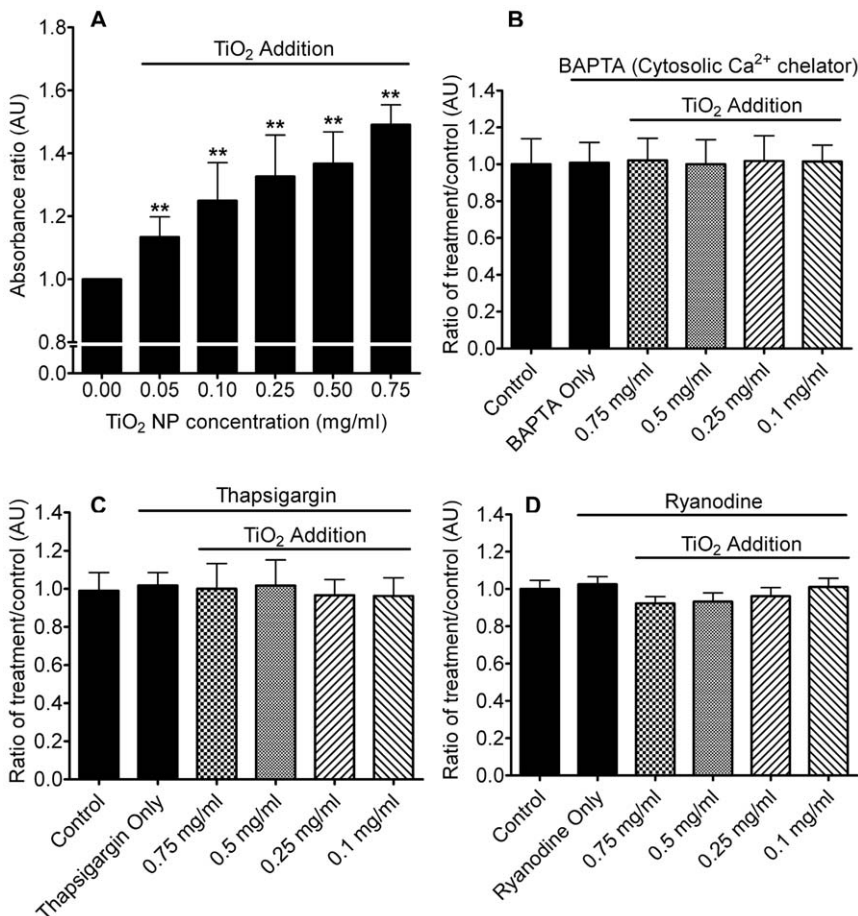


Figure 4. Measurement of mucin secretion triggered by TiO_2 NPs. Cells were treated with TiO_2 NP concentrations ranging from 0.05 mg/ml –0.75 mg/ml. Figure 4A) shows the relative quantification of mucin secreted after TiO_2 stimulation under normal conditions ($n \geq 7$, $**P < 0.005$), 4B) in the presence of BAPTA-AM (50 μ M) ($n \geq 9$), 4C) with pre-treatment of thapsigargin (100 nM) ($n \geq 8$), 4D), and with ryanodine (100 μ M) ($n \geq 5$). doi:10.1371/journal.pone.0016198.g004

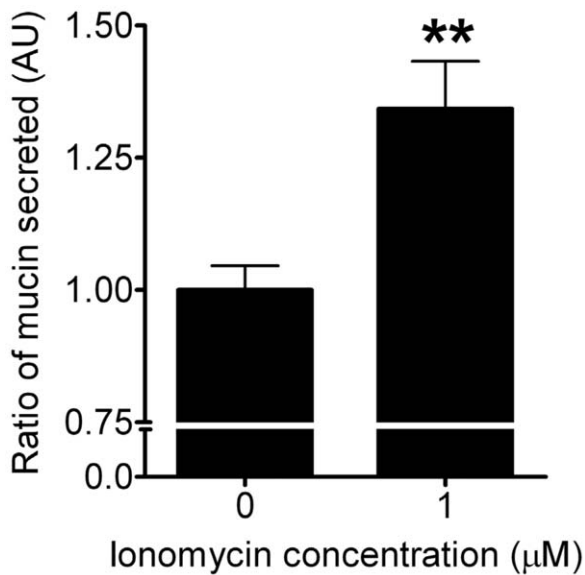


Figure 5. Mucin secretion in response to ionomycin application (positive control, $n \geq 3$). Concentration of ionomycin used was 1 μM . doi:10.1371/journal.pone.0016198.g005

Discussion

Recently, an increasing number of reports have shown that airborne particulate pollution found in both the ambient and working environments, particularly TiO_2 NPs, can exacerbate airway diseases [1,2,3,4,5,6,10,11,38]. Aggravated clinical manifestations of COPD, CF and asthma may include intensified symptoms of mucociliary transport impairment and mucus hypersecretion [15,39]. The resultant accumulation of thick obstructive mucus usually occupies airway lumen, thereby limiting airflow and leading to morbidity [15,39]. Despite documentations of TiO_2 -induced cellular nanotoxicity effects, pulmonary inflammatory responses and emphysema-like pathology [12], whether TiO_2 NPs can directly trigger mucin secretion has not been resolved. In this study, we demonstrate that TiO_2 NPs can stimulate mucin secretion from bronchial epithelial ChaGo-K1 cells via a Ca^{2+} -dependent pathway.

Our study showed that TiO_2 NPs can induce mucin secretion that increases as a function of TiO_2 NP concentration (Fig. 4A). The TiO_2 concentration range used in our study is consistent with previous reports representing the concentration found in ambient and nanotechnology industries [30,40,41,42]. While NP exposure has been long associated with increasing mucin synthesis due to goblet cell hyperplasia [13], our study indicates that TiO_2 NPs can directly trigger mucin secretion in the airway.

It has been well established that intracellular Ca^{2+} plays a vital role in stimulus-secretion coupling [43]. Previous reports have documented that an elevated $[\text{Ca}^{2+}]_C$ precedes mucin granule exocytosis [17]. NP exposure has been shown to trigger an intracellular Ca^{2+} increase in various cells; therefore, we examined the cellular Ca^{2+} signaling pathway involved during TiO_2 stimulation [25,28,44]. At TiO_2 concentrations of 0.5, 0.75, and 1 mg/ml, there was a sustained elevation in $[\text{Ca}^{2+}]_C$. At lower doses (0.05, 0.1 and 0.25 mg/ml), the $[\text{Ca}^{2+}]_C$ increased gradually within the 1st minute (Fig. 1B). Our data demonstrated that TiO_2 NPs induced a concentration dependent increase in $[\text{Ca}^{2+}]_C$, which is consistent with results from the mucin secretion measurements (Fig. 4A).

The stimulus-induced intracellular Ca^{2+} signal can be evoked by the entry of Ca^{2+} through voltage-gated Ca^{2+} channels, or by the

release of Ca^{2+} from intracellular Ca^{2+} stores [43,45,46]. Previous researches have suggested that extracellular Ca^{2+} influx plays an important role in the elevated $[\text{Ca}^{2+}]_C$ during NP stimulation [25,27,28,47]. Data from experiments performed in Ca^{2+} -free Hanks' solution confirmed that $[\text{Ca}^{2+}]_C$ failed to increase when treated with TiO_2 NPs (Fig. 2A). To characterize the nature of the Ca^{2+} influx induced by TiO_2 NPs, we first evaluated the effect of cadmium chloride (CdCl_2), a general Ca^{2+} channel blocker [34,48]. Figure 2B shows that the $[\text{Ca}^{2+}]_C$ remained low and relatively unchanged with CdCl_2 . Secondly, nifedipine, a widely used L-type Ca^{2+} channel blocker, markedly diminished the increase in $[\text{Ca}^{2+}]_C$ (Fig. 2C). The effect of nifedipine implies that TiO_2 NPs can activate L-type voltage gated Ca^{2+} channels, allowing extracellular Ca^{2+} influx into the cytosol. This observation is consistent with previous reports showing that ultrafine carbon black and ZnO NP-induced $[\text{Ca}^{2+}]_C$ elevation can also be attenuated by nifedipine [27,28]. In addition, several reports have suggested that oxidative stress induced by NPs can exert an impact on the intracellular Ca^{2+} signaling pathway and that the activity of Ca^{2+} channels may be altered by ROS [27,28,44]. Results from Figure 2E showed that NAC significantly reduced the rising $[\text{Ca}^{2+}]_C$ generated by TiO_2 NPs. Huang et al, has also demonstrated that NAC can attenuate the intracellular Ca^{2+} level when challenged with ZnO NPs [27]. Our results support the idea that NAC and other antioxidants may be effective in reducing NP-instigated mucin hypersecretion. NPs such as TiO_2 can damage cell membrane integrity by possible lipid peroxidation [27,31], thereby creating pores on the lipid bilayer [49] that may allow the transient influx of extracellular Ca^{2+} . Our data further demonstrated that co-administration of TiO_2 NPs and fluorescent calcein dye lead to intracellular leakage and the permeation efficiency increased in a TiO_2 concentration dependent manner (Fig. 2D). Calcein has also been previously utilized to evaluate the efficacy of peptides in causing membrane perturbation [50]. Our result suggests that the possible membrane perturbation/transient pore formation induced by TiO_2 NPs allows an extracellular Ca^{2+} influx and may account for the portion of Ca^{2+} that can not be completely abolished by blocking L-type Ca^{2+} channels with nifedipine.

Increasing the $[\text{Ca}^{2+}]_C$ of human goblet cells has been shown to trigger degranulation [17]. We used BAPTA (cytosolic Ca^{2+} chelator) to test whether the increase in Ca^{2+} induced by TiO_2 NPs could stimulate mucin exocytosis. It is evident that BAPTA significantly inhibited mucin exocytosis (Fig. 4B), indicating that TiO_2 NPs can elicit a $[\text{Ca}^{2+}]_C$ increase, thereby leading to mucin secretion.

Besides the external Ca^{2+} source (Hanks' solution), the ER is one of the major internal Ca^{2+} stores. Figures 3A and 4C revealed that when the ER Ca^{2+} had been depleted by pretreatment with thapsigargin, the TiO_2 NP-induced $[\text{Ca}^{2+}]_C$ failed to increase significantly, and the subsequent mucin secretion was abolished. Our data indicates that the ER plays a critical role in relaying TiO_2 -induced Ca^{2+} signaling. CICR is a positive feedback mechanism where the ER amplifies a small increase in $[\text{Ca}^{2+}]_C$, (e.g. due to voltage-gated Ca^{2+} influx [22]), with the activation of RYRs that will lead to the release of more Ca^{2+} from the ER [19,20]. Previous studies have shown that through activation of RYRs with Ca^{2+} , CICR can generate an overall increase in $[\text{Ca}^{2+}]_C$ [20,21,22]. Our data showed that ryanodine inhibited a continual rise in $[\text{Ca}^{2+}]_C$ when applying TiO_2 NPs (Fig. 3B). Therefore, it is indicative that the TiO_2 -instigated increase in $[\text{Ca}^{2+}]_C$ was also CICR dependent. The effect of ryanodine was further demonstrated by the lack of mucin secretion under TiO_2 NP stimulation (Fig. 4D).

In summary, our study indicates that cellular exposure to TiO₂ NPs can activate membrane L-type Ca²⁺ channels, induce ROS production and possibly disrupt the cellular membrane. Influx of extracellular Ca²⁺ into the cytoplasm raises [Ca²⁺]_C, which in turn can trigger ryanodine receptors on the ER to release ER resident Ca²⁺ via the CICR mechanism. A sufficient increase in the cytosolic Ca²⁺ level results in subsequent mucin secretion. More importantly, our results provide a direct link between airborne particulate matters and the pathogenesis of chronic airway diseases involving mucus hypersecretion and airway obstruction. In addition, we demonstrate that once thought inert and harmless TiO₂ NPs can indeed interfere with intracellular Ca²⁺ signaling, possibly leading to pathological states.

References

- Alfaro-Moreno E, Nawrot TS, Nemmar A, Nemery B (2007) Particulate matter in the environment: pulmonary and cardiovascular effects. *Curr Opin Pulm Med* 13: 98–106.
- Gwinn MR, Vallyathan V (2006) Nanoparticles: health effects—pros and cons. *Environ Health Perspect* 114: 1818–1825.
- Sethi S (2004) New developments in the pathogenesis of acute exacerbations of chronic obstructive pulmonary disease. *Curr Opin Infect Dis* 17: 113–119.
- Atkinson RW, Anderson HR, Sunyer J, Ayres J, Baccini M, et al. (2001) Acute effects of particulate air pollution on respiratory admissions: results from APHEA 2 project. *Air Pollution and Health: a European Approach*. *Am J Respir Crit Care Med* 164: 1860–1866.
- Ling SH, van Eeden SF (2009) Particulate matter air pollution exposure: role in the development and exacerbation of chronic obstructive pulmonary disease. *Int J Chron Obstruct Pulmon Dis* 4: 233–243.
- Stone V (2000) Environmental air pollution. *Am J Respir Crit Care Med* 162: S44–47.
- Boezen M, Schouten J, Rijcken B, Vonk J, Gerritsen J, et al. (1998) Peak expiratory flow variability, bronchial responsiveness, and susceptibility to ambient air pollution in adults. *Am J Respir Crit Care Med* 158: 1848–1854.
- Card JW, Zeldin DC, Bonner JC, Nestmann ER (2008) Pulmonary applications and toxicity of engineered nanoparticles. *Am J Physiol Lung Cell Mol Physiol* 295: L400–411.
- Johnston HJ, Hutchison GR, Christensen FM, Peters S, Hankin S, et al. (2009) Identification of the mechanisms that drive the toxicity of TiO₂ particulates: the contribution of physicochemical characteristics. *Part Fibre Toxicol* 6: 33.
- Ahn MH, Kang CM, Park CS, Park SJ, Rhim T, et al. (2005) Titanium dioxide particle-induced goblet cell hyperplasia: association with mast cells and IL-13. *Respir Res* 6: 34.
- Garabrant DH, Fine LJ, Oliver C, Bernstein L, Peters JM (1987) Abnormalities of pulmonary function and pleural disease among titanium metal production workers. *Scand J Work Environ Health* 13: 47–51.
- Chen HW, Su SF, Chien CT, Lin WH, Yu SL, et al. (2006) Titanium dioxide nanoparticles induce emphysema-like lung injury in mice. *FASEB J* 20: 2393–2395.
- Hyun JS, Lee BS, Ryu HY, Sung JH, Chung KH, et al. (2008) Effects of repeated silver nanoparticles exposure on the histological structure and mucins of nasal respiratory mucosa in rats. *Toxicol Lett* 182: 24–28.
- Voynow JA, Rubin BK (2009) Mucins, mucus, and sputum. *Chest* 135: 505–512.
- Rogers DF (2007) Physiology of airway mucus secretion and pathophysiology of hypersecretion. *Respir Care* 52: 1134–1146; discussion 1146–1139.
- Verdugo P (1990) Goblet cells secretion and mucogenesis. *Ann Rev Physiol* 52: 157–176.
- Abdullah LH, Conway JD, Cohn JA, Davis CW (1997) Protein kinase C and Ca²⁺ activation of mucin secretion in airway goblet cells. *Am J Physiol* 273: L201–210.
- Nguyen T, Chin WC, Verdugo P (1998) Role of Ca²⁺/K⁺ ion exchange in intracellular storage and release of Ca²⁺. *Nature* 395: 908–912.
- Berridge MJ, Bootman MD, Roderick HL (2003) Calcium signalling: dynamics, homeostasis and remodelling. *Nat Rev Mol Cell Biol* 4: 517–529.
- Ashby MC, Craske M, Park MK, Gerasimenko OV, Burgoyne RD, et al. (2002) Localized Ca²⁺ uncaging reveals polarized distribution of Ca²⁺-sensitive Ca²⁺ release sites: mechanism of unidirectional Ca²⁺ waves. *J Cell Biol* 158: 283–292.
- Meissner G (1994) Ryanodine receptor/Ca²⁺ release channels and their regulation by endogenous effectors. *Annu Rev Physiol* 56: 485–508.
- Solovyova N, Veselovsky N, Toescu EC, Verkhatsky A (2002) Ca²⁺ dynamics in the lumen of the endoplasmic reticulum in sensory neurons: direct visualization of Ca²⁺-induced Ca²⁺ release triggered by physiological Ca²⁺ entry. *Embo J* 21: 622–630.
- Mogami H, Zhang H, Suzuki Y, Urano T, Saito N, et al. (2003) Decoding of short-lived Ca²⁺ influx signals into long term substrate phosphorylation through activation of two distinct classes of protein kinase C. *J Biol Chem* 278: 9896–9904.
- Zhu H, Hille B, Xu T (2002) Sensitization of regulated exocytosis by protein kinase C. *Proc Natl Acad Sci U S A* 99: 17055–17059.
- Brown DM, Donaldson K, Borm PJ, Schins RP, Dehnhardt M, et al. (2004) Calcium and ROS-mediated activation of transcription factors and TNF- α cytokine gene expression in macrophages exposed to ultrafine particles. *Am J Physiol Lung Cell Mol Physiol* 286: L344–353.
- Brown DM, Hutchison L, Donaldson K, Stone V (2007) The effects of PM10 particles and oxidative stress on macrophages and lung epithelial cells: modulating effects of calcium-signaling antagonists. *Am J Physiol Lung Cell Mol Physiol* 292: L1444–1451.
- Huang CC, Aronstam RS, Chen DR, Huang YW (2009) Oxidative stress, calcium homeostasis, and altered gene expression in human lung epithelial cells exposed to ZnO nanoparticles. *Toxicol In Vitro* 24: 45–55.
- Stone V, Tuinman M, Vamvakopoulos JE, Shaw J, Brown D, et al. (2000) Increased calcium influx in a monocytic cell line on exposure to ultrafine carbon black. *Eur Respir J* 15: 297–303.
- Dahiya R, Kwak KS, Byrd JC, Ho S, Yoon WH, et al. (1993) Mucin synthesis and secretion in various human epithelial cancer cell lines that express the MUC-1 mucin gene. *Cancer Res* 53: 1437–1443.
- Chen E, Ruvalcaba M, Araujo L, Chapman R, Chin WC (2008) Ultrafine titanium dioxide nanoparticles induce cell death in human bronchial epithelial cells. *Journal of Experimental Nanoscience* 3: 171–183.
- Gurr JR, Wang AS, Chen CH, Jan KY (2005) Ultrafine titanium dioxide particles in the absence of photoactivation can induce oxidative damage to human bronchial epithelial cells. *Toxicology* 213: 66–73.
- Chen EY, Wang YC, Chen CS, Chin WC (2010) Functionalized Positive Nanoparticles Reduce Mucin Swelling and Dispersion. *PLoS One* 5: e15434.
- Chen EY, Yang N, Quinton PM, Chin WC (2010) A New Role for Bicarbonate in Mucus Formation. *Am J Physiol Lung Cell Mol Physiol*.
- Nguyen T, Chin WC, O'Brien JA, Verdugo P, Berger AJ (2001) Intracellular pathways regulating ciliary beating of rat brain ependymal cells. *J Physiol* 531: 131–140.
- Kawasaki S, Takizawa H, Takami K, Desaki M, Okazaki H, et al. (2001) Benzene-extracted components are important for the major activity of diesel exhaust particles: effect on interleukin-8 gene expression in human bronchial epithelial cells. *Am J Respir Cell Mol Biol* 24: 419–426.
- Edwards DA, Prausnitz MR, Langer R, Weaver JC (1995) Analysis of Enhanced Transdermal Transport by Skin Electroporation. *Journal of Controlled Release* 34: 211–221.
- Kemp PA, Sugar RA, Jackson AD (2004) Nucleotide-mediated mucin secretion from differentiated human bronchial epithelial cells. *Am J Respir Cell Mol Biol* 31: 446–455.
- Stone V, Johnston H, Clift MJ (2007) Air pollution, ultrafine and nanoparticle toxicology: cellular and molecular interactions. *IEEE Trans Nanobioscience* 6: 331–340.
- Randell SH, Boucher RC, Grp UNCVL (2006) Effective mucus clearance is essential for respiratory health. *Am J Respir Cell Mol Biol* 35: 20–28.
- Barlow PG, Clouter-Baker A, Donaldson K, Maccallum J, Stone V (2005) Carbon black nanoparticles induce type II epithelial cells to release chemotaxins for alveolar macrophages. *Part Fibre Toxicol* 2: 11.
- Sayes CM, Wahi R, Kurian PA, Liu Y, West JL, et al. (2006) Correlating nanoscale titania structure with toxicity: a cytotoxicity and inflammatory response study with human dermal fibroblasts and human lung epithelial cells. *Toxicol Sci* 92: 174–185.
- Zhang AP, Sun YP (2004) Photocatalytic killing effect of TiO₂ nanoparticles on Ls-174-t human colon carcinoma cells. *World J Gastroenterol* 10: 3191–3193.
- Petersen CC, Toescu EC, Petersen OH (1991) Different patterns of receptor-activated cytoplasmic Ca²⁺ oscillations in single pancreatic acinar cells: dependence on receptor type, agonist concentration and intracellular Ca²⁺ buffering. *Embo J* 10: 527–533.
- Donaldson K, Stone V, Borm PJ, Jimenez LA, Gilmour PS, et al. (2003) Oxidative stress and calcium signaling in the adverse effects of environmental particles (PM10). *Free Radic Biol Med* 34: 1369–1382.

Acknowledgments

The authors thank Profs. Pedro Verdugo and Paul Quinton for their support and encouragement during the preparation of this manuscript.

Author Contributions

Conceived and designed the experiments: EYTC MG YCW CSC WCC. Performed the experiments: EYTC MG YCW. Analyzed the data: EYTC MG YCW. Contributed reagents/materials/analysis tools: EYTC MG YCW CSC. Wrote the paper: EYTC WCC.

45. Berridge MJ, Irvine RF (1984) Inositol triphosphate, a novel second messenger in cellular signal transduction. *Nature* 312: 315–321.
46. Berridge MJ, Irvine RF (1989) Inositol phosphates and cell signalling. *Nature* 341: 197–205.
47. Brown DM, Hutchison L, Donaldson K, MacKenzie SJ, Dick CA, et al. (2007) The effect of oxidative stress on macrophages and lung epithelial cells: the role of phosphodiesterases 1 and 4. *Toxicol Lett* 168: 1–6.
48. Boulton CL, O'Shaughnessy CT (1991) The Effect of Calcium Channel Antagonists on Spontaneous and Evoked Epileptiform Activity in the Rat Neocortex In Vitro. *Eur J Neurosci* 3: 992–1000.
49. Kelly CV, Leroueil PR, Orr BG, Banaszak Holl MM, Andricioaei I (2008) Poly(amidoamine) dendrimers on lipid bilayers II: Effects of bilayer phase and dendrimer termination. *J Phys Chem B* 112: 9346–9353.
50. Chou HT, Wen HW, Kuo TY, Lin CC, Chen WJ (2010) Interaction of cationic antimicrobial peptides with phospholipid vesicles and their antibacterial activity. *Peptides* 31: 1811–1820.